IMAGE RETARGETING USING STABLE PATHS

Hélder P. Oliveira
Faculdade de Engenharia, Universidade do Porto, Porto, Portugal
helder.oliveira@fe.up.pt

Jaime S. Cardoso
INESC Porto, Faculdade de Engenharia, Universidade do Porto, Porto, Portugal
jaime.cardoso@inescporto.pt

Keywords: Image processing, Image retargeting, Image resizing, Stable paths.

Abstract: Media content adaptation is the action of transforming media files to adapt to device capabilities, usually related to mobile devices that require special handling because of their limited computational power, small screen size and constrained keyboard functionality. Image retargeting is one of such adaptations, transforming an image into another with different size. Tools allowing the author to imagery once and automatically retarget that imagery for a variety of different display devices are therefore of great interest. The performance of these algorithms is directly related with the preservation of the most important regions and features of the image.
In this work, we introduce an algorithm for automatically retargeting images. We explore and extend a recently proposed algorithm on the literature. The central contribution is the introduction of the stable paths for image resizing, improving both the computational performance and the overall quality of the resulting image. The experimental results confirm the potential of the proposed algorithm.

1 INTRODUCTION

Increasingly, our computing and communications infrastructure is evolving to support images and video. The recent diversity and versatility of mobile displays, such as PDAs and cellular phones, have enlarged the importance of adaptation of images for these devices. Traditional image manipulation techniques, such as scaling and cropping, lead to a degradation of image quality and important loss of information when automatically applied to images with multiple objects. In such techniques, valuable image area in the target image may be wasted with unimportant regions between important features. Content aware retargeting algorithms try to change the image size while preserving the most important information in it.

In this work we present a novel scheme to resize an image. Our algorithm repeatedly carves out multiple lines simultaneously. To do this, we draw on the work by Avidan and Shamir on seam carving (Avidan and Shamir, 2007). Analogous to their approach, we identify low energy seams that are carved out from the image. The seams are not restricted to be straight but rather follow the contours of low-gradient regions in the image. In this work we extend and explore their approach in two main directions. Firstly, the use of stable paths instead of the shortest path improves the computational performance of the method by selecting multiple seams simultaneously. Furthermore, this option also has the advantage of spreading more evenly the removed seams on the image, improving the overall quality. Secondly, the design of the weights on the graph resulting from the image is generalized to depend nonlinearly on the gradient value. Moreover, we also distinguish, in terms of cost, pair of pixels 4-neighbourhood-connected from pixels only connected under 8-neighbourhoods. This improvement in the weight design enhances further the final performance.

After reviewing the state of the art in image retargeting, we introduce in Section 3 the concept of stable paths in a graph and present a computationally efficient algorithm for determining them. The experimental work reported at the end of the communication includes a thorough testing on real images, where the original method in (Avidan and Shamir, 2007) is compared with the extensions proposed in this work.

2 RELATED WORKS

Before describing in detail the proposed method for image retargeting it is instructive to examine the current state of the art.

A non-photorealistic algorithm was proposed in (Setlur et al., 2005) to adapt automatically images for small sized displays with different sizes and/or aspect ratios, while preserving the important features in the image. This is achieved by first decomposing the image in a background layer and foreground objects. Then, all important zones are temporally cropped and the other parts are removed from the image. The final image is obtained by pasting the important zones, with the rest of the image obtained by resizing some parts using inpainting (Harrison, 2001).

In (Liu and Gleicher, 2005) and (Liu and Gleicher, 2006) the authors propose a method for image and video retargeting, respectively. Their method presents a tradeoff between image resizing and image cropping. The method consists on finding the Region-of-Interest (ROI) of the image and constructing a novel Fisheye-View warp that applies a linear scaling function in each dimension of the image. Basically, in this method the information on the ROI is preserved and the rest of the image is warped. In the video application they use a combination of the image and saliency maps to find the ROI. After this operation, cropping, virtual pan and shot cuts are used to resize the image.

In (Gal et al., 2006) is presented a method for inhomogeneous 2D texture mapping by a feature mask to the general problem of warping, that preserves some parts of the image specified by the user. The feature-aware texture warping is done by applying a formulation based on Laplacian editing technique.

An automatic non-uniform global warping was employed by (Wolf et al., 2007) in a problem of video retargeting. The algorithm starts by analyzing the frame to detect important zones and then shrinks less important regions. The analysis of the frames is based on local saliency, and object and motion detection.

The technique of cropping the important zones and then resizing them to obtain the desired aspect ratio was applied in (Tao et al., 2007) to a problem of video retargeting. In (Chen and Sen, 2008) the authors use graph cuts to find and remove low gradient sheets, for video summarization applications.

An approach for the summarization of visual data for images and videos is proposed in (Simakov et al., 2008). The authors propose a measure to quantify how “good” is a visual summary. This measure can be applied to compare two images or two videos sequences with different sizes. This is useful to improve some objective function within an optimization process, to generate good visual summaries or to compare quantitatively and evaluate visual summaries produced by different methods.

An important work in image retrieving was recently presented by Avidan (Avidan and Shamir, 2007), and improved by Rubinstein (Rubinstein et al., 2008) for video retargeting. In (Avidan and Shamir, 2007) the authors create an operator called *seam carving* that permits the reduction and enlarging of images. A *seam* was defined as an optimal 8-connected path of pixels between opposing margins of the image, where optimally is determined using an image energy function. The algorithm preserves the image structure by removing more low energy pixels than high energy pixels. The computation of the optimal seam is based on an efficient dynamic programming algorithm. In (Rubinstein et al., 2008) the authors extend the work for video. There, the dynamic programming had to be replaced by graph cuts, suitable for 3D volumes. A novel energy function was also introduced, improving the visual quality of both videos and images.

The principal problem of the algorithm in (Avidan and Shamir, 2007; Rubinstein et al., 2008) is related with the lower performance when applied to images with big sizes. The algorithm is slow because only one line is discarded per iteration.

3 A STABLE PATH APPROACH FOR IMAGE RESIZING

In the work to be detailed, the image grid is considered as a graph with pixels as nodes and arcs connecting neighbouring pixels. The weight of each arc, $w(p,q)$, is a function of pixels values and pixels relative positions. A path from vertex (pixel) v_1 to vertex (pixel) v_n is a list of unique vertices $v_1, v_2, \ldots, v_n$, with v_i and v_{i+1} corresponding to neighbour pixels. The total cost of a path is the sum of each arc weight in the path $\sum_{i=2}^{n} w(v_{i-1}, v_i)$.

A path from a source vertex v to a target vertex u is said to be a *shortest path* if its total cost is minimum among all v-to-u paths. The distance between a source vertex v and a target vertex u on a graph, $d(v,u)$, is the total cost of a shortest path between v and u.

A path from a sub-graph Ω_1 to a sub-graph Ω_2 is said to be a shortest path between Ω_1 and Ω_2 if its total cost is minimum among all $v \in \Omega_1$-to-$u \in \Omega_2$ paths. The distance from a sub-graph Ω_1 to a sub-graph Ω_2, $d(\Omega_1, \Omega_2)$, is the total cost of a shortest path between Ω_1 and Ω_2:

$$d(\Omega_1, \Omega_2) = \min_{v \in \Omega_1, u \in \Omega_2} d(v,u). \quad (1)$$

3.1 Algorithm Outline

For completeness and to help introducing the proposed method, we summarize here the method in (Avidan and Shamir, 2007), in which we build on. The presentation will rely on height reduction only; the necessary adaptations for width reduction or image enlarging should be clear at the end.

To reduce the height of an image by one pixel, one needs to remove one and only one pixel in each column. Moreover, in order to prevent discontinuities, the removed pixels should be connected. Therefore, we are allowed to remove only any connected path from the left to the right margins, without zig zagging back and forth (Avidan and Shamir, 2007). Formally, let I be an $N_1 \times N_2$ image and define an admissible path to be

$$\mathbf{s} = \{(x, y(x))\}_{x=1}^{N_1} \text{ , s.t. } \forall x \; |y(x) - y(x-1)| \leq 1,$$

where y is a mapping $y : [1, \cdots, N_1] \rightarrow [1, \cdots, N_2]$. That is, an admissible path is an 8-connected path of pixels in the image from left to right, containing one, and only one, pixel in each column of the image.

In (Avidan and Shamir, 2007) the authors propose to remove the path with least energy. Toward that end a weight (= energy) is defined for each arc connecting neighbour pixels; then the optimal path is the minimum-cost path connecting the two lateral margins. This optimal path can be found using dynamic programming. The first step is to traverse the image from the second column to the last column and compute the cumulative minimum cost C for all possible connected staff lines for each entry (i, j):

$$C(i,j) = \min \begin{cases} C(i-1, j-1) & + \quad w(p_{i-1,j-1}; p_{i,j}) \\ C(i-1, j) & + \quad w(p_{i-1,j}; p_{i,j}) \\ C(i-1, j+1) & + \quad w(p_{i-1,j+1}; p_{i,j}) \end{cases},$$

where $w(p_{i,j}; p_{l,m})$ represents the weight of the edge incident with pixels at positions (i, j) and (l, m). At the end of this process,

$$\min_{j \in \{1, \cdots, N_2\}} C(N_1, j)$$

indicates the end of the minimal connected path. Hence, in the second step, one backtrack from this minimum entry on C to find the path of the optimal staff.

3.1.1 Design of the Weight Function

It is important to call the attention for the first improvement over (Avidan and Shamir, 2007). In (Avidan and Shamir, 2007), the authors define a weight (energy) on each pixel. In here we put the weight on the arc connecting two neighbour pixels. Had we defined the arc's weight as the average of the pixels' weight, our formulation would resume to the previous. But by putting the weight on the arc we have now the flexibility to distinguish a path over an arc connecting 4-neighbour pixels from an arc connecting 8-neighbour pixels, penalising the latter over the former. The weight of each arc is a function of pixels values *and* pixels relative positions.

In this work we set

$$w(p_{i,j}; p_{l,m}) = \begin{cases} f(p_{i,j}, p_{l,m}) \\ \qquad \text{if } p_{i,j}, p_{l,m} \text{ are 4-neighbours} \\ \sqrt{2} f(p_{i,j}, p_{l,m}) \\ \qquad \text{if } p_{i,j}, p_{l,m} \text{ are 8-neighbours} \end{cases}$$

Note that is important to set $f(p_{i,j}, p_{l,m})$ strictly greater than zero so that $\sqrt{2} f(p_{i,j}, p_{l,m})$ is strictly greater than $f(p_{i,j}, p_{l,m})$.

3.2 Stable Paths on a Graph[1]

Assume one wants to decrease the height of the image by several pixels. This can be approached by successively finding and removing the shortest path from the left to the right margin of the image. A preferable solution would be to find multiple paths in a single iteration. The stable path method allows us to do precisely that.

Before moving to the formal definition of a stable path on a graph, it is instructive to motivate the concept by considering a hypothetical, simplified 9×10 image. The graph corresponding to such image is represented in Figure 1. The design of the weight function will be considered next; for now, it suffices to know that black pixels represent pixels with low cost (energy), likely resulting from points with low gradient.

The shortest path between the left and right margins (sub-graphs Ω_1 and Ω_2) is the path corresponding to the fourth row, entirely through black pixels. By following the strategy just delineated, one could reduce the height by four pixels in four iterations, sequentially. Nonetheless, although only one path corresponds to the shortest path, it is visible multiple 'almost optimal' paths. The stable path concept provides a means to find all of such paths simultaneously.

Definition. A path $\mathcal{P}_{s,t}$ is a stable path between regions Ω_1 and Ω_2 if $\mathcal{P}_{s,t}$ is the shortest path between $s \in \Omega_1$ and the whole region Ω_2, and $\mathcal{P}_{s,t}$ is the shortest path between $t \in \Omega_2$ and the whole region Ω_1.

[1]A first incursion into stable paths is already present in (Cardoso et al., 2008), in the context of medical imaging; here we provide, arguably, a cleaner presentation.

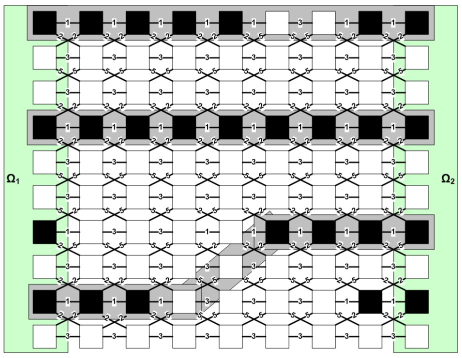
Figure 1: Stable paths on a toy example.

Note that the concept of stable path is valid for any graph and any two sub-graphs in general. The computation of the stable paths on the toy example of Figure 1 provides the three paths gray-highlighted in the figure.

In Figure 2(b) the shortest paths between *each point* on the left margin and the *whole* right margin are traced. Likewise, Figure 2(c) shows the shortest paths between *each point* on the right margin and the *whole* left margin. The set of stable paths between both margins result as the set of paths present in both figures, as illustrated in Figure 2(d).

Although the computation of the stable paths may be expensive in general graphs, the computation in the graph derived from an image under the setting adopted in Section 3.1 has only roughly twice the complexity of the shortest path computation presented in the same Section. Noticing that the procedure delineated in Section 3.1 actually gives the shortest path between the whole left margin Ω_1 and each point on the right margin Ω_2, the first step on the computation of the stable path corresponds verbatim to the computation of the shortest path presented on Section 3.1. In a second step one repeats the same procedure, traversing now the graph from the right column to the left. At the end of this process, if the two endpoints of a direct and reverse path coincide, we are in the presence of a stable path.

Noticing that the two steps of computing the shortest paths in both directions can done in parallel and most personal computers are nowadays dual cores, the computation of the stable paths takes essentially the same time as the shortest path computation. Finally, when the number of stable paths is less than the number of lines to be removed, one just repeats the procedure after removing the stable paths found; when the number of stable paths is larger than the necessary, one just keeps the shortest stable paths. While the description has focused on height reduction, the same mechanism applies for width reduction or image enlarging, totally in line with the adaptations in (Avidan and Shamir, 2007).

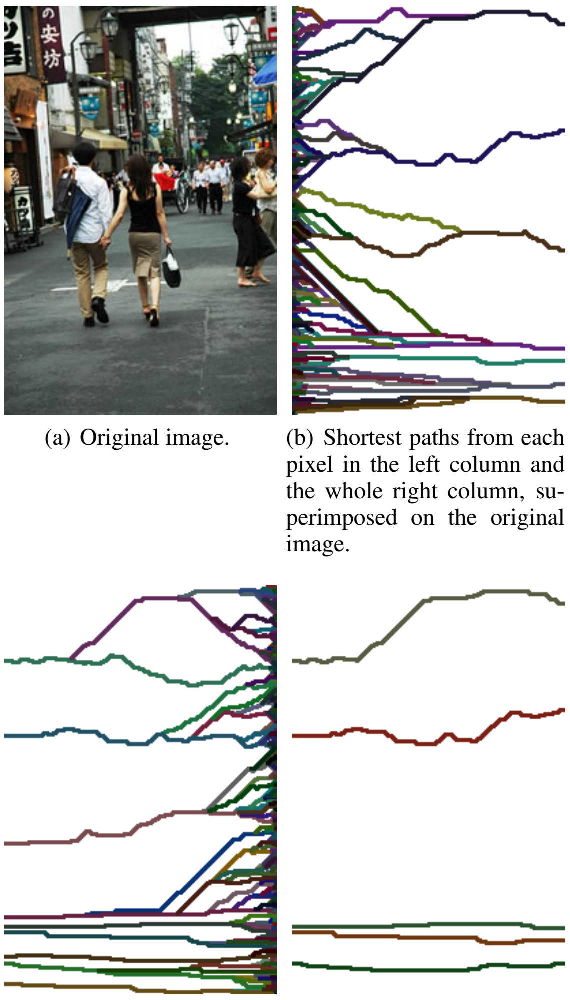
(a) Original image. (b) Shortest paths from each pixel in the left column and the whole right column, superimposed on the original image.

(c) Shortest paths from each pixel in the right column and the whole left column, superimposed on the original image. (d) Resulting stable paths.

Figure 2: Exemplification of stable paths for Figure 2(a).

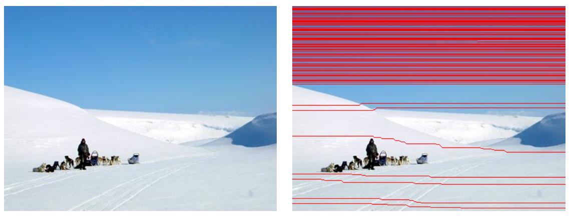
(a) Original image. (b) Original image stable paths superimposed.

Figure 3: Staff lines for Figure 3(a).

Summing up, two main advantages accrue from the replacement of the sequential search of the shortest path by the search of stable paths: multiple lines can be computed in a single iteration, saving on the computational time; the stable path approach tends to spread the lines over the image, as observed in Figure 2 and Figure 3.

Indeed, while the shortest paths tend to be all clustered in a single, gradient-free zone of the image, the stable paths are usually found in several zones of the image.

4 RESULTS

The proposed methodology was applied to a set of 36 images. Only the luminance information was used in the analysis. The weight of an arc is based on the energy of the incident pixels. Like in (Avidan and Shamir, 2007), the energy function is derived from the gradient information. Our gradient model is based on the Sobel operator. The Sobel operator is applied on the x and y directions; from the computed values, E_x and E_y, the magnitude of the gradient is estimated as $E = \sqrt{E_x^2 + E_y^2}$, as exemplified in Figure 4. Although more general setting could have been adopted, we fixed the weight of an arc as monotonically increasing function of the average energy of the incident pixels (or $\sqrt{2}$ times that value, for 8-neighbour pixels): $f(p_{i,j}, p_{l,m}) = \hat{f}(\frac{E_{i,j}+E_{l,m}}{2})$.

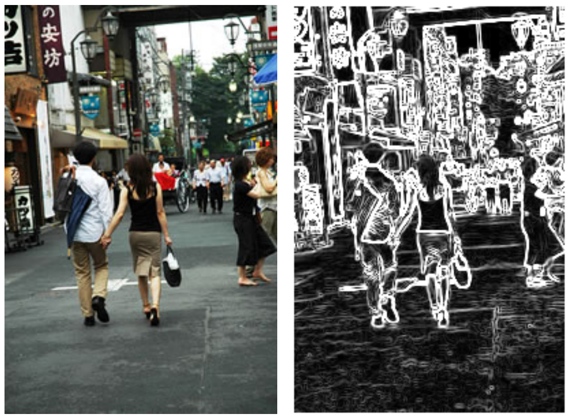
(a) Original image. (b) Gradient image.

Figure 4: Gradient based on the Sobel operator.

Weights were assigned based on an power law:

$$\hat{f}(E) = \delta + 255\left(\frac{E}{255}\right)^n, \quad \delta, n \in \Re$$

The parameters δ and n were experimentally tuned, yielding $\delta = 32$ and $n = 2$. For comparison purposes

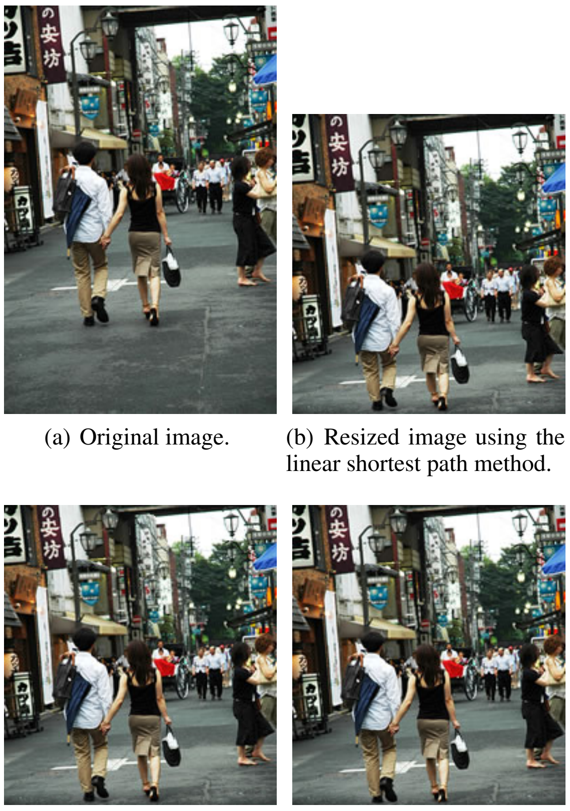
(a) Original image. (b) Resized image using the linear shortest path method.

(c) Resized image using the linear stable path method. (d) Resized image using the nonlinear stable path method.

Figure 5: Results of the different resizing methods when applied to image E.

we also evaluated the linear weight ($n = 1$). Five different methods are experimentally compared:

1. **Linear Shortest Path.** A slightly improved version of the method in (Avidan and Shamir, 2007), with the incorporation of the $\delta > 0$ parameter, to ensure that the cost of 8-neighbour pixels is larger than 4-neighbour pixels. This method discards a single line per iteration.
2. **Linear Stable Path.** Based on stable paths to discard multiple line per iteration but using the linear weight function ($n = 1$).
3. **Nonlinear Shortest Path** The method of (Avidan and Shamir, 2007) discarding a single line per iteration but using the nonlinear weight function ($n = 2$).
4. **Nonlinear Stable Path.** Based on stable paths to discard multiple line per iteration and using the nonlinear weight function ($n = 2$).
5. **Scaling.** Standard scaling, with Lanczos filtering.

The new size of each image was subjectively chosen to make visible differences between the different

Table 1: Results obtained using different resize methods.

Image	Height	Discarded Lines	Number Iterations		
			Linear and nonlinear shortest path	Linear stable path	Nonlinear stable path
A	230	35	35	20 (57%)	12 (34%)
B	230	35	35	14 (40%)	5 (14%)
C	288	80	80	42 (53%)	42 (53%)
D	230	10	10	10 (100%)	6 (60%)
E	300	80	80	58 (73%)	49 (61%)
F	200	30	30	21 (70%)	13 (43%)
G	300	60	60	26 (43%)	25 (42%)
H	300	75	75	44 (59%)	41 (55%)
I	230	80	80	51 (64%)	53 (66%)
J	230	110	110	75 (68%)	61 (55%)
K	230	60	60	30 (50%)	34 (57%)
L	180	60	60	37 (62%)	29 (48%)
M	220	60	60	27 (45%)	16 (27%)
N	1536	150	150	46 (31%)	6 (4%)
O	1944	100	100	29 (29%)	15 (15%)
P	800	100	100	48 (48%)	14 (14%)
Q	600	70	70	34 (49%)	30 (43%)
R	800	90	90	33 (37%)	27 (30%)
S	355	80	80	58 (73%)	10 (13%)
T	274	70	70	43 (61%)	38 (54%)
U	400	100	100	41 (41%)	36 (36%)
V	402	70	70	31 (44%)	23 (33%)
W	290	30	30	10 (33%)	4 (13%)
X	375	30	30	29 (97%)	27 (90%)
Y	504	70	70	32 (46%)	21 (30%)
Z	411	130	130	59 (45%)	56 (43%)
AA	332	35	35	18 (51%)	22 (63%)
AB	350	110	110	60 (55%)	63 (57%)
AC	375	50	50	31 (62%)	25 (50%)
AD	385	50	50	27 (54%)	14 (28%)
AE	300	65	65	30 (46%)	33 (51%)
AF	480	50	50	20 (40%)	19 (38%)
AG	324	40	40	36 (90%)	23 (58%)
AH	504	150	150	24 (16%)	15 (10%)
AI	319	150	150	57 (38%)	8 (5%)
AJ	428	150	150	38 (25%)	27 (18%)
Average				(53%)	(39%)

methods. The results can be found in the Table 1. The percentage values are the fraction of iterations necessary by the stable path algorithms relative to the total number of iteration required by the shortest path methods (that matches the number of removed lines).

It can be observed that the proposed algorithm has a very interesting performance. The use of the stable paths reduced the number of iterations and the corresponding computational complexity. The simultaneous use of a nonlinear weight function and the stable path method reduced further the number of iterations required to resize the image.

In a second experiment we evaluated the impact on quality of the use of stable paths to resize images. It is important to confirm if we are trading off quality for computational performance.

In Figures 5 and 6 it is presented the results obtained with the linear shortest path method and the linear and nonlinear stable path method. It is possible to observe that the stable path method attain a better quality; the principal visual improvement can be seen on people appearance.

From the analysis of the results reported in Figure 7, it is possible to conclude that the nonlinear weight function presents a better behaviour than the linear weight. The principal visual impact can be seen on the horizon of the scenery. Furthermore, is possible to observe, by comparing Figure 7(c) and 7(d), that the stable path algorithm outperforms the shortest path algorithm. The resized image using our method

(a) Original image.

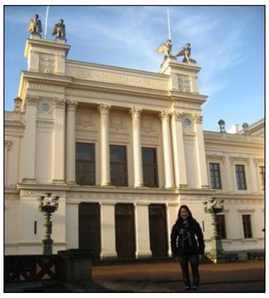
(b) Resized image using the linear shortest path method.

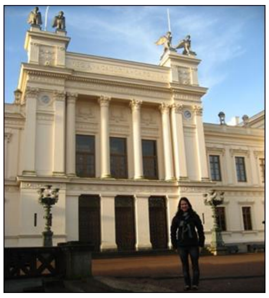
(c) Resized image using the linear stable path method.

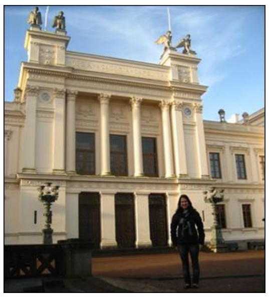
(d) Resized image using the nonlinear stable path method.

Figure 6: Results of the different resizing methods when applied to image *V*.

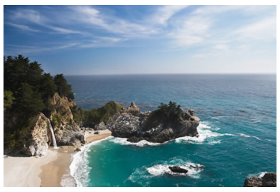
(a) Original image.

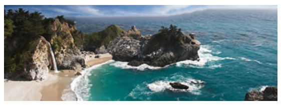
(b) Resized image using the linear shortest path method.

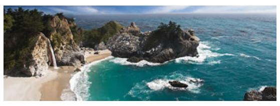
(c) Resized image using the nonlinear shortest path method.

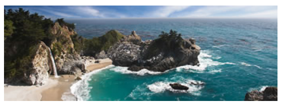
(d) Resized image using the nonlinear stable path method.

Figure 7: Results of the different resizing methods when applied to image *J*.

seems more natural: in Figure 7(c) the sky is very compacted when compared with Figure 7(d).

In Figures 8 and 9 we can observe that our algorithm can be simultaneously faster and with better quality than the version in (Avidan and Shamir, 2007), both on small sized images and big sizes image, respectively.

(a) Original image.

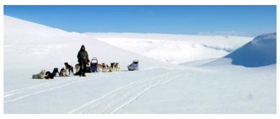
(b) Resized image using the linear shortest path method.

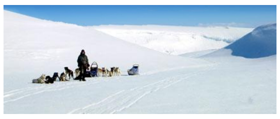
(c) Resized image using the nonlinear shortest path method.

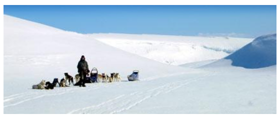
(d) Resized image using the nonlinear stable path method.

Figure 8: Results of the different resizing methods when applied to image *AI*.

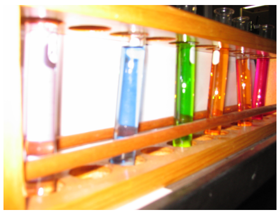
(a) Original image.

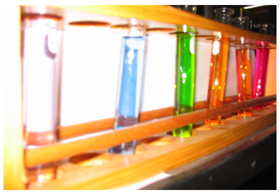
(b) Resized image using the linear shortest path method.

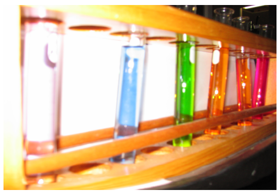
(c) Resized image using the nonlinear shortest path method.

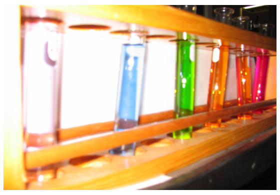
(d) Resized image using the nonlinear stable path method.

Figure 9: Results of the different resizing methods when applied to image *N*.

The lack of metrics to perform this evaluation objectively, led us to create a panel of observers to evaluate subjectively the output of the different algorithms. Besides confirming the results already demonstrated, an interesting conclusion was that, in some images, the traditional rescaling continues to be preferable.

5 CONCLUSIONS

We presented an algorithm for content-aware image resizing. The proposed method is an improvement over an already established method in the literature. We exploit the concept of stable paths to enhance both the computational speed and the quality of the resulting image. The generalization of the weight function of the graph derived from the image further improved the quality results. Though the experimental results have focused on image reduction only, the method is straightforwardly applied to image enlarging, image amplification and object removal. We intend now to generalize and adapt the concept of stable paths for video retargeting.

REFERENCES

Avidan, S. and Shamir, A. (2007). Seam carving for content-aware image resizing. *ACM Trans. Graph.*, 26(3):10.

Cardoso, J. S., Teixeira, L. F., and Cardoso, M. J. (2008). Automatic breast contour detection in digital photographs. In *Proceedings of the International Conference on Health Informatics (HEALTHINF 2008)*, volume 2, pages 91–98.

Chen, B. and Sen, P. (2008). Video carving. In *Short Papers Proceedings of Eurographics*.

Gal, R., Sorkine, O., and Cohen-Or, D. (2006). Feature-aware texturing. In *Proceedings of Eurographics Symposium on Rendering*, pages 297–303.

Harrison, P. (2001). A non-hierarchical procedure for re-synthesis of complex textures. In *WSCG 2001 Conference proceedings*, pages 190–197. WSCG.

Liu, F. and Gleicher, M. (2005). Automatic image retargeting with fisheye-view warping. In *UIST '05: Proceedings of the 18th annual ACM symposium on User interface software and technology*, pages 153–162, New York, NY, USA. ACM.

Liu, F. and Gleicher, M. (2006). Video retargeting: automating pan and scan. In *MULTIMEDIA '06: Proceedings of the 14th annual ACM international conference on Multimedia*, pages 241–250, New York, NY, USA. ACM.

Rubinstein, M., Shamir, A., and Avidan, S. (2008). Improved seam carving for video retargeting. *ACM Transactions on Graphics (SIGGRAPH)*, 27(3).

Setlur, V., Takagi, S., Raskar, R., Gleicher, M., and Gooch, B. (2005). Automatic image retargeting. In *MUM '05: Proceedings of the 4th international conference on Mobile and ubiquitous multimedia*, pages 59–68, New York, NY, USA. ACM.

Simakov, D., Caspi, Y., Shechtman, E., and Irani, M. (2008). Summarizing visual data using bidirectional similarity. In *IEEE Conference on Computer Vision and Pattern Recognition*, pages 1–8.

Tao, C., Jia, J., and Sun, H. (2007). Active window oriented dynamic video retargeting. In *Proceedings of the Workshop on Dynamical Vision*.

Wolf, L., Guttmann, M., and Cohen-Or, D. (2007). Non-homogeneous content-driven video-retargeting. *In IEEE 11th International Conference on Computer Vision*, pages 1–6.